Nonlinear Finite Element Analysis for Punching Shear Resistance of Steel Fibers High Strength Reinforced Concrete Slabs

Dr. Eyad K. Sayhood
Building and Construction Engineering Department, University of Technology/Baghdad
Dr. Samer P. Yaakoub
Building and Construction Engineering Department, University of Technology/Baghdad
Hussien Fadhil Hussien
Building and Construction Engineering Department, University of Technology/Baghdad
Email: hfh_52@yahoo.com

Received on: 18/9/2013 & Accepted on: 6/2/2014

ABSTRACT

This study is devoted to investigate the punching shear resistance of high strength reinforced concrete slabs with steel fibers by using the well-known (P3DNFEA), a non-linear finite element program for three-dimensional analysis of reinforced concrete structure.

Nine high strength reinforced concrete slabs with steel fibers and one without steel fibers, have been analyzed in the present study. The finite element solutions are compared with the available experimental data. In general, accepted agreement between the numerical results and the experimental results has been obtained.

Parametric studies have been carried out to investigate the effect of concrete compressive strength, steel fiber content, amount of steel rebars, slab depth and column dimensions on the behavior and ultimate strength of reinforced concrete slabs.

The numerical analysis indicated that the increase in the concrete compressive strength (f'_c) from 40 to 80 MPa has led to an increase in the strength by 69% and 84% for slabs without and with 0.5% steel fibers respectively. The numerical analysis indicated that by using 2.0% steel fibers, the ultimate capacity is increased by 81.7%, compared to a slab without fibers.

Also, the finite element solution revealed that increasing the longitudinal reinforcement ratio in the slab from 1% to 2% led to an increase in the ultimate shear strength of about 57%.

Keywords: Punching Shear ,Slab, Steel Fiber ,Finite Element ,Nonlinear

https://doi.org/10.30684/etj.32.6A.6
2412-0758/University of Technology-Iraq, Baghdad, Iraq

التحليل اللاخطي بالعناصر المحددة لمقاومة القص الثاقب للبلاطات الخرسانية المسلحة عالية المقاومة والمعززة بالالياف الفولاذية

الخلاصة

في هذا البحث تم دراسة مقاومة القص الثاقب للبلاطات الخرسانية المسلحة العالية المقاومة و المعززة بالالياف الفولاذية بواسطة التحليل اللاخطي ثلاثي الابعاد بطريقة العناصر المحددة باستخدام البرنامج الشائع. (P3DNFEA) في هذه الدراسة تم تحليل تسعة بلاطات خرسانية عالية المقاومة والمعززة بالالياف الفولاذية وبلاطة واحدة خالية من الالياف الفولاذية. قورنت النتائجالمستحصلة من طريقة العناصر المحددة مع النتائج العملية. بشكل عام حصل توافق مقبول بين النتائج التحليلية والعملية.
المتغيرات التي تم دراستها هي تأثير مقاومة الانضغاط للخرسانة، محتوى الالياف الفولاذية، كمية حديد التسليح، عمق البلاطة وابعاد الاعمدة على تصرف وتحمل البلاطات الخرسانية.
اشارت النتائج التحليلية الى زيادة مقاومة الانضغاط للخرسانة من (40) الى (80) ميغا باسكال أدت الى زيادة المقاومة بنسبة (69%)، (84%) للبلاطات الخالية من الالياف والبلاطات التي تحتوي على نسبة (0.5%) من الالياف على التوالي.
ان استخدام نسبة (2%) من الالياف الفولاذية ادى الى زيادة مقاومة القص القصوى للبلاطات بنسبة (81.7%) مقارنة مع البلاطات التي لاتحتوي على الالياف، بينما زيادة نسبة حديد التسليح الطولي من (1%) الى (2%) ادى الى زيادة مقاومة القص القصوى بحدود (57%).

Notation

d_f	Diameter of fiber
f'_c	Uniaxial compressive strength of concrete
f'_{cf}	Uniaxial compressive strength of fibrous concrete
f_{tf}	Uniaxial tensile strength of fibrous concrete
L_f	Fiber length
N_f	Number of fibers per unit area
V_f	Volume fraction of fibers
α_1 , α_2	Tension-stiffening parameter
β	Shear retention factor or material constant.
λ	Compressive strength reduction factor of concrete
σ_0	Effective stress at onset of plastic deformation
ε_{cr}	Cracking tensile strain in concrete
ε_{tf}	Tensile strain at peak tensile stress
ε_{cuf}	Fibrous Concrete Ultimate strain in compression

INTRODUCTION

A flat-plate slab system can be defined as a slab with uniform thickness supported on the columns without beams, drop panels or column capitals. Conventionally, the reinforced concrete flat-plate systems are generally used for lightly loaded structures, such as residential or office buildings with relatively short spans. Flat-plates have been widely used due to the reduced construction cost associated with the simple formwork and simple arrangement of flexural reinforcement. An additional advantage of a flat-plate is a reduced building story height that results in more usable space in building for a given or limited height (1).

The undesirable suddenness and the catastrophic nature of the failure can be formed at the connection between the slab and the column which is called punching shear failure. A typical punching shear failure in reinforced concrete begins with the formation of flexural hinges (yield lines) around the perimeter of the loaded area, these hinges develop as a result of the moment caused in the slab by the applied load. This moment then begins to produce radial cracks that extend outward from the area of loading to the perimeter of the slab. Failure of the slab occurs when the diagonal tension cracks intersect the radial cracks and produce a cone of failure(2).

Two characteristics, however, have been limited the use of high strength concrete (HSC): it is brittle and weak in tension. Recently, for improving these deficiencies, instead of reinforcement bars, different kind of fibers are used (3).Research findings in the last decade clearly establish that the ductility of certain structural members can be greatly enhanced with the use of fibers. In addition, fibers are generally favor improvements in first crack and ultimate member strength, impact resistance, and shear resistance. The deficiencies of ordinary reinforced concrete in the form of micro-cracks, which cannot be corrected by bar reinforcement, can be remedied to a significant extent by fiber reinforcement.

Addition of randomly oriented fiber in plain concrete helps to bridge and arrest the cracks formed in the brittle concrete under applied stresses, and enhances the ductility and energy absorption properties of the composite (4).

The ability of steel fibers to enhance shear strength of concrete is attributed to the possible transfer of tensile stresses across crack surfaces, that is known as crack-bridging, when steel fibers are incorporated. This phenomenon permits fiber reinforced concrete to have more ductile failure than normal concrete (5).When fibers are added in a slab-column connection, the residual strength of the slab-column connection after the formation of punching shear crack increases significantly, due to the enhanced structural integrity between the slab and the column (6).

Finite Element Model

In the present research work, a full three - dimensional finite element idealization has been used. This idealization gives accurate simulation for geometry, type of failure and location of reinforcing bars. The 20-node quadratic brick element shown in Fig. (1) is adopted to represent concrete in the present study.

The reinforcement representation that is used in this study is the embedded representation, Fig. (1). The reinforcing bar is considered to be an axial member built into the concrete element. Perfect bond was assumed to occur between the concrete and the reinforcing bars. The reinforcing bars were assumed to be capable of transmitting axial force only.

The numerical integration is generally carried out using the 27(3x3x3) point Gaussian type integration rule. The nonlinear equations of equilibrium have been solved using an incremental-iterative technique operating under load control. The nonlinear solution algorithm that is used in this research work is the modified Newton –Raphson method in which the stiffness matrix is updated at the2nd, 12th, 22nd, ...etc. iterations of each increment of loading .

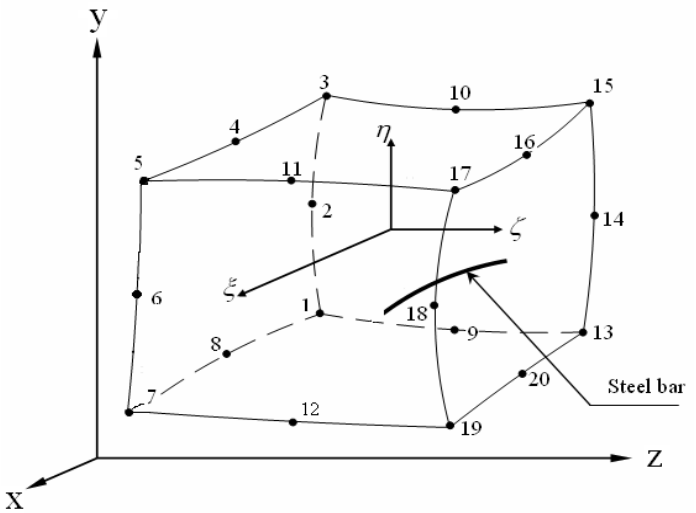

Figure (1) Twenty-node isoparametric brick element. (11)

Material Model Adopted in the Analysis

Behavior in Compression:

In compression, the behavior of concrete is simulated by an elastic-plastic work hardening model followed by a perfectly plastic response, which is terminated at the onset of crushing. The growth of subsequent loading surfaces is described by an isotropic hardening rule. A parabolic equivalent uniaxial stress-strain curve has been used to represent the work hardening stage of behavior and the plastic straining is controlled by an associated flow rule. The concrete strength under multidimensional state of stress is a function of the state of stress and cannot be predicted by simple tensile, compressive and shearing stress independent of each other. So the state of stress must be scaled by an appropriate yield criterion to convert it to equivalent stress that could be obtained from simple experimental test. The yield criterion that has been used successfully by many investigators (7),(8) can be expressed as :

$$f(\{\sigma\}) = (\alpha I_1 + 3\beta J_2)^{0.5} = \sigma_0 \qquad \ldots (1)$$

where α and β are material parameters which are dependent on the type of concrete, mainly on the volume fraction of fiber V_f , and their values are shown in Table (1) (9),(10).I_1 is the first stress invariant and J_2 is the second deviatoric stress invariant. σ_0 is an equivalent effective stress at the onset of plastic deformation which can be determined from a uniaxial compression test.

Table (1) Values of α and β for different fiber ratios (11)

Fiber contentV_f%	α	β
0.0	0.3546798 σ_0	1.3546798
0.5	1.0993042σ_0	2.0993042
1.0	1.4900526σ_0	2.4900526
1.5	1.760526σ_0	2.7960526
2	2.278595σ_0	3.0108

In a reinforced concrete member, a significant degradation in compressive strength can result due to the presence of transverse tensile straining after cracking. In the present study, Vecchio et, al. models are used for high strength concrete (HSC) (9) members, which illustrates the use of the reduction factor, λ . The compressive reduction factor, λ , for HSC is given as:

$$\lambda = \frac{1}{1 + K_c.K_f} \qquad \ldots (2)$$

where K_c is a factor representing the effect of the transverse cracking and straining and K_f is a factor representing the effect of concrete compressive strength f'_c.

$$K_c = 0.35(\varepsilon_1/\varepsilon_3 - 0.28)^{0.8} \qquad \ldots (3)$$

and

$$K_f = 0.1825\sqrt{f'_c} \geq 1.0 \qquad \ldots (4)$$

where ε_1 is the tensile strain in the direction normal to the crack and ε_3 is the compressive strain in the direction parallel to the crack.

Behavior in Tension:

In tension, linear elastic behavior prior to cracking is assumed. Cracking is governed by the attainment of a maximum principal stress criterion. A fixed smeared crack model has been used to simulate the behavior of concrete in tension with a tension-stiffening model to represent the retained post-cracking tensile stresses. The degradation of the shear strength of concrete due to cracking is accounted for by employing a shear-retention model. A smeared crack model with fixed orthogonal cracks is assumed to represent the cracked sampling point. The post-cracking tensile stress-strain relations, Fig. (2),[11],[12] and the reduction in shear modulus with increasing tensile strain Fig. (3),[13] have been adopted in the present work. The tensile strain at peak tensile stress ε_{tf} is given by:

$$\varepsilon_{tf} = \varepsilon_t (1 + 0.35 N_f . d_f . L_f) \quad \ldots (5)$$

Where

N_f : is the number of fiber per unit area; given by:

$$N_f = \eta_0 \left[\frac{4V_f}{\pi . d_f} \right] \quad \ldots (6)$$

Behavior of Steel Fiber Reinforced Concrete

In compression, an empirical equation for peak strain value in uniaxial compression of high strength fiber reinforced concrete (ε_{pf}) suggested by Al- Azzawi[14] is adopted in the present study as:

$$\varepsilon_{pf} = 0.00212 + 0.001 * V_f * \frac{L_f}{d_f} \quad \ldots (7)$$

In this study, an empirical equations for (f'_{cf})suggested by Bunni[15] is adopted and is given by :

$$f'_{cf} = 1.43 \ (f'_c)^{0.941} . \left((L_f / d_f) V_f . K_f \right)^{0.054} \quad \ldots (8)$$

According to test results reported in reference [16] the concrete peak value of the tensile stress of high strength fiber reinforced concrete (f'_{tf}) is proposed in terms of compressive strength of normal concrete (f'_c)and fiber volume fraction ($V_f$in percent) as follows:

$$f_{tf} = 0.58 \sqrt{f'_c} + 302 V_f \quad \ldots (9)$$

$$E_c = 3320\sqrt{f'_c} + 6900 \quad \text{For } 21 \text{ MPa} < f'_c < 81 \text{ MPa} \qquad \ldots(10)$$

$$\varepsilon_{cuf} = (3011 + 2295V_f) \times 10^{-6} \qquad \ldots(11)$$

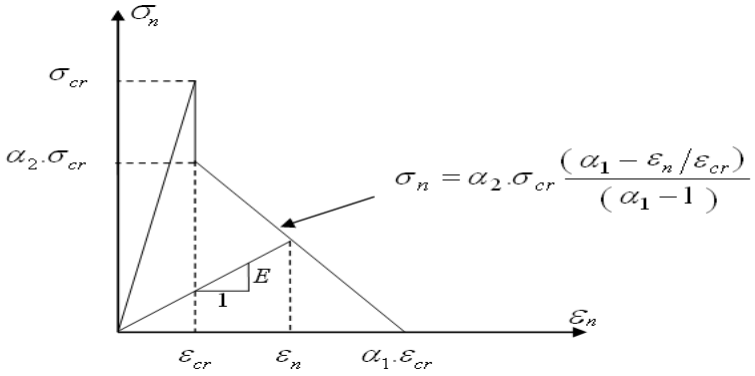

a) Plain concrete (11)

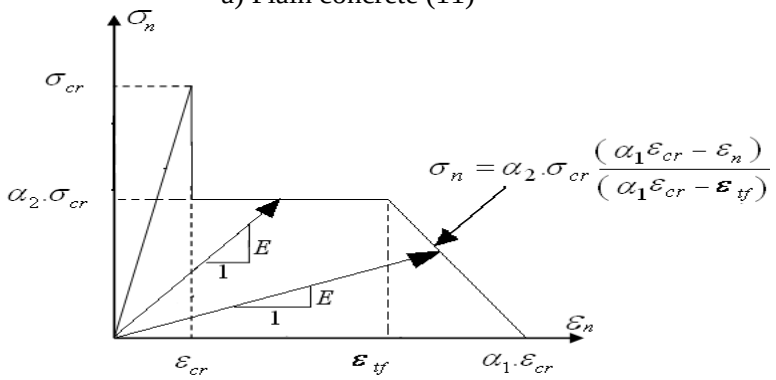

b) Fiber reinforced concrete (12)

Figure (2) Post-cracking models for cracked concrete.

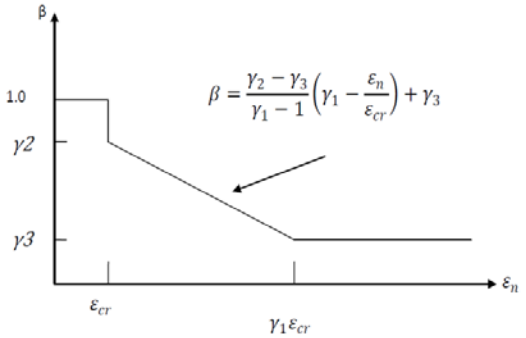

Figure (3) Shear retention model for cracked concrete (11).

Numerical Example

Description of Test Specimens:

Abdulhameed (3) tested experimentally fourteen high strength steel fiber reinforced concrete slabs . Eight of these slabs were chosen for the finite element analysis. The slabs were simply supported along all four edges by using a special manufactured frame with the corners free to rise.

All the slabs were 800 mm square, 60 mm thick and loaded through a central column 100x100 mm. They were provided with a two-way flexural reinforcement consisting of eighteen, 6 mm-diameter deformed steel bars in each direction. Column stubs were reinforced with eight deformed steel bars of 6 mm diameter, cut to length 10 mm less than the height of the column, and two, 6mm diameter, deformed steel ties 60 mm apart. The overall dimensions of the specimens and the arrangement of the reinforcement are given in Fig.(4) and Fig.(5).

The same type of fibers was used throughout the test program. The fibers were straight plain, 40mm in length and 0.3 mm in diameter making an aspect ratio (L_f/d_f) of133, . The steel fibers had an ultimate tensile strength of512 MPa. Different amounts of steel fibers $V_{(f)}$were used in the test program.

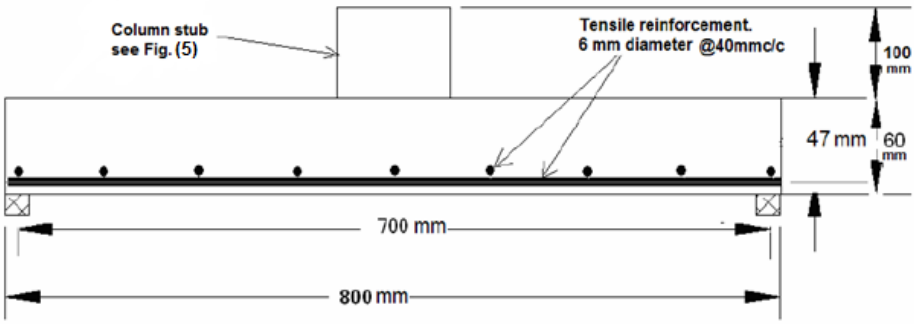

Figure (4) Dimensions of test slabs and details of reinforcement.

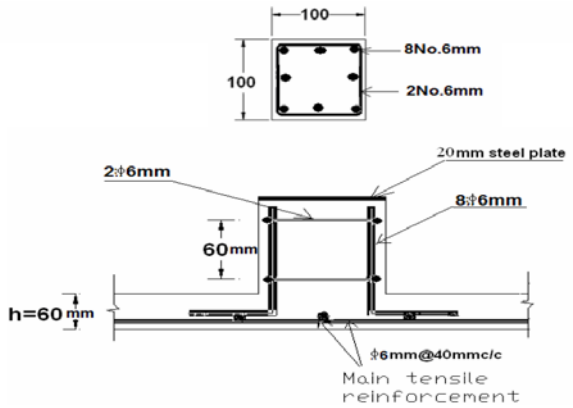

Figure (5) Reinforcement of column stubs.

Finite Element Idealization and Material Properties:

By taking into consideration the advantage of loading and geometric symmetry, only one-quarter of the specimen has been used in the finite element analysis. The selected quarter was discretized into 51 quadratic brick elements. The external concentrated load was modeled as nodal forces applied on the column stub. The finite element mesh, boundary conditions, and loading arrangement are shown in Fig. (6). Material properties and the adopted additional material parameters are listed in Table (2).

The finite element analysis has been carried out using the 27-point integration rule, with a convergence tolerance of (5%). The modified Newton-Raphson method, in which the stiffness matrix is updated at 2^{nd},12^{th},22^{nd} …etc. iterations of each increment of loading, was adopted as a nonlinear solution algorithm. Non-uniform increments of applied loads have been used. Large increments of loading were used at early stages of loading, and then smaller increments of loading were used at stages close to the ultimate load.

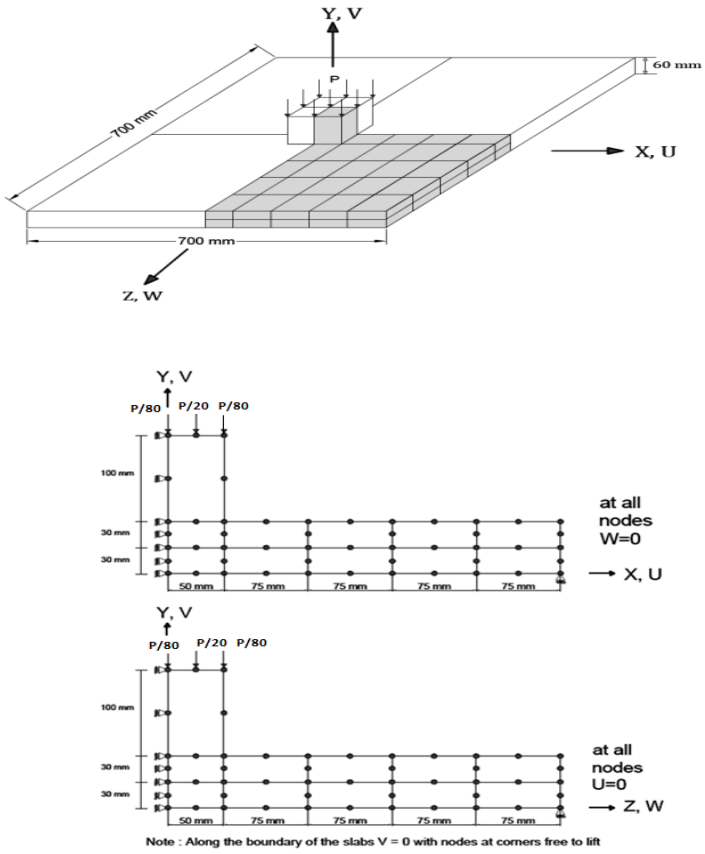

Figure (6) Finite element idealization, symmetry and boundary conditions used for Abdulhameed slabs.

Results of Analysis:

The experimental and numerical load-deflection curves for slabs S11 to S24 are shown in Fig. (7) and Fig. (8). Generally, the numerical solutions are in accepted agreement with the experimental results throughout the entire range of the behavior for each tested slab.

The predicted response is approximately similar to the experimental response throughout the pre-cracking stages of behavior. While, it becomes slightly stiffer throughout the post-cracking stages of behavior. However, the ultimate shear capacity obtained from the numerical analysis is almost equal to the experimental ultimate shear capacity. The computed failure loads for all slabs are close to the corresponding experimental collapse load as listed in Table (3).

Parametric Studies

To investigate the effect of some important material and solution parameters on the nonlinear finite element analysis of high strength steel fiber reinforced concrete slabs which fail by punching, slab S12 has been chosen to carry out the parametric study. This study helps to clarify the effect of various parameters that have been considered on the behavior and ultimate load of the analyzed slabs.

Influence of Grade of Concrete

In order to study the influence of using different values of concrete compressive strength (f'_c) on the behavior of reinforced concrete slabs with and without steel fibers, slab S21 without steel fibers was analyzed for different values of (f'_c). The selected values of the concrete compressive strength used in this study were 40, 50, 60, 70 and 80 MPa. Fig. (9) shows the effect of grade of concrete on the response of slab S21 represented by the load – deflection curves. This figure reveals that as the concrete compressive strength increases, the post - cracking stiffness and the predicted ultimate shear capacity are significantly increased.

While to investigate the effect of compressive strength of fibrous concrete (f'_{cf}), slab S12 (V_f = 0.5) was analyzed by using the same different values of (f'_c) used for slab S21 after applying equation (8),suggested by Bunni[15], to obtain the values of (f'_{cf}), as shown in Table (4). Fig. (10) shows the effect of grade of fibrous concrete on the response of slab S12 represented by the load-deflection curves. This figure reveals that as the concrete compressive strength increases, the post-cracking stiffness and the predicted ultimate shear capacity are significantly increased. The numerical ultimate load capacity for slabs S21 and S12 obtained from this study are listed in Tables (5)and(6), respectively.

Table (2) Material properties and material parameters used for Abdulhameed slabs.

Slab		S11	S12	S13	S14	S21	S22	S23	S24
Concrete	Volume fraction of fibers V_f %	0.5	0.5	0.5	0.5	0.0	0.25	0.75	1
	Compressive strength f'_{cf}(MPa)	35.36	49.14	55.06	65.13	42.19	48.76	52.38	53.26
	Young modulus[17],E_c* (GPa)	26.64	30.17	31.54	33.69	28.46	30.08	30.93	31.13
	Tensile strength f_{tf} ** (MPa)	4.96	5.57	5.81	6.19	3.77	4.81	6.46	7.25
	Poisson's ratio υ †	0.2	0.2	0.2	0.2	0.2	0.2	0.2	0.2
	Uniaxial crushing strain[18], $\varepsilon_{cu\,f}$ ***	0.004159	0.004159	0.004159	0.004159	0.003011	0.003585	0.004732	0.005306
Steel	Yield stress f_y(MPa)	670	670	670	670	670	670	670	670
	Young modulus E_s (GPa)	200	200	200	200	200	200	200	200
	Steel ratio , ρ (%)	1.5	1.5	1.5	1.5	1.5	1.5	1.5	1.5
Column size *c* (mm x mm)		100x100	100x100	100x100	100x100	100x100	100x100	100x100	100x100
Numerical parameters	**Tension-stiffening parameters†**								
	α_1	10	10	10	10	8	8	13	15
	α_2	0.5	0.5	0.5	0.5	0.5	0.5	0.5	0.5

† Assumed values

$$*E_c = 3320\sqrt{f'_c} + 6900 \quad \text{For } 21 \text{ MPa} < f'_c < 81 \text{ MPa} \qquad \ldots(10)$$

$$** \ f_{tf} = 0.58\sqrt{f'_c} + 302V_f \qquad \ldots(9)$$

$$*** \ \varepsilon_{cuf} = (3011 + 2295V_f) \times 10^{-6} \qquad \ldots(11)$$

Table (3) Comparison between the experimental and numerical load capacities for Abdulhameed tested slabs.

Slab	V_f %	V_u Exp. (kN)	V_u FEM (kN)	V_u FEM/V_u Exp. %
S11	0.5	89.5	77.044	86.1
S12	0.5	102.5	91.91	89.7
S13	0.5	129.5	120.24	92.8
S14	0.5	141	129.7	91.9
S21	0.0	93.25	84.34	90.4
S22	0.25	98	92.84	94.7
S23	0.75	125.5	116.34	92.7
S24	1	138	129.16	93.6

Table (4) Values of compressive strength of fibrous concrete used for analyzing slab S12

f'_cMPa	40.0	50.0	60.0	70.0	8.0
f'_{cf} * MPa	43.36	53.49	63.50	73.42	83.25

$$* \ f'_{cf} = 1.43 \left(f'_c\right)^{0.941} . \left(\left(L_f / d_f\right) V_f . K_f\right)^{0.054} \quad \text{.....(8)}$$

Table (5) Numerical ultimate loads of slab S21 (V_f= 0.0%) for various grades of concrete ($f'c$).

Concrete compressive strength (MPa)	FEM	Exp.	FEM			
	40	42.19	50	60	70	80
Ultimate load (kN)	76.35	93.25	87.5	103.23	115.34	129.48
Final deflection (mm)	8.53	10.05	9.12	10.08	10.45	11.58

Table (6) Numerical ultimate loads of slab S12 (V_f = 0.5%) for various grades of concrete ($f'c$).

Concrete compressive strength (MPa)	FEM	Exp.	FEM			
	43.36	49.14	53.49	63.50	73.42	83.25
Ultimate load (kN)	82.54	102.5	101.5	114.47	135.2	152.36
Final deflection (mm)	8.13	10.20	9.65	10.82	13.05	14.92

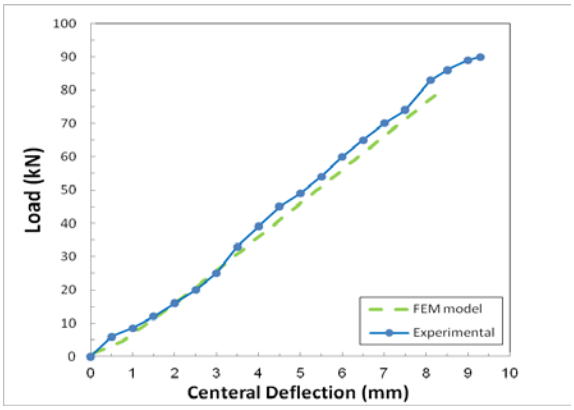

Slab S11

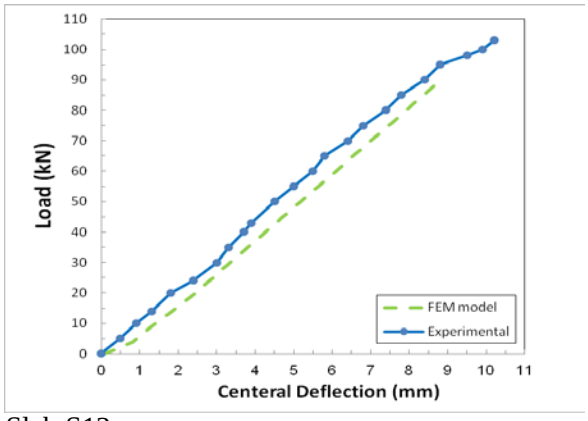

Slab S12

Figure(7). Continuation

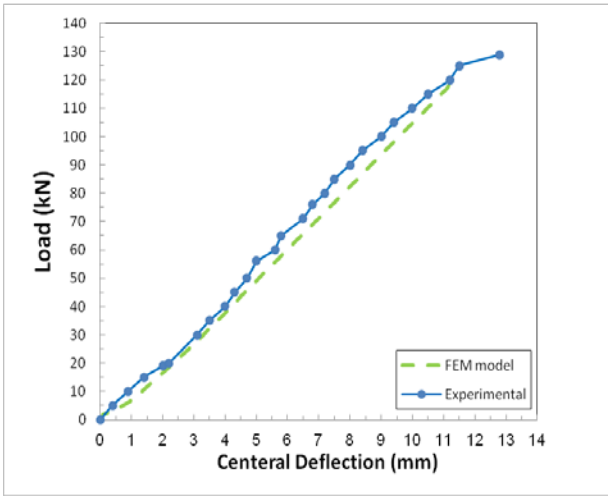

Slab S13

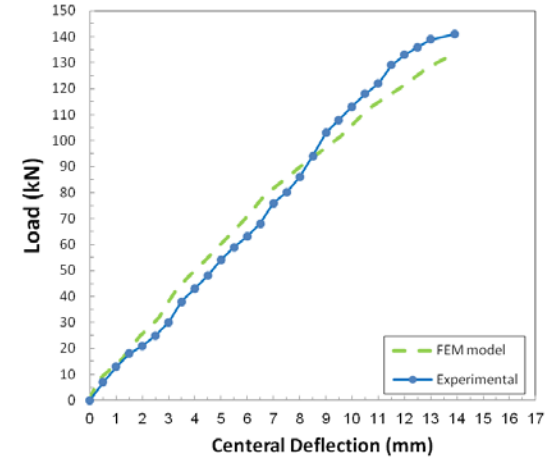

Slab S14

Figure(7). Continuation

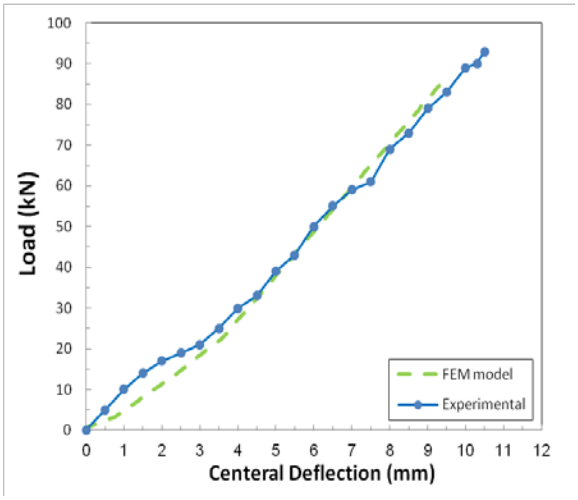

Slab S21

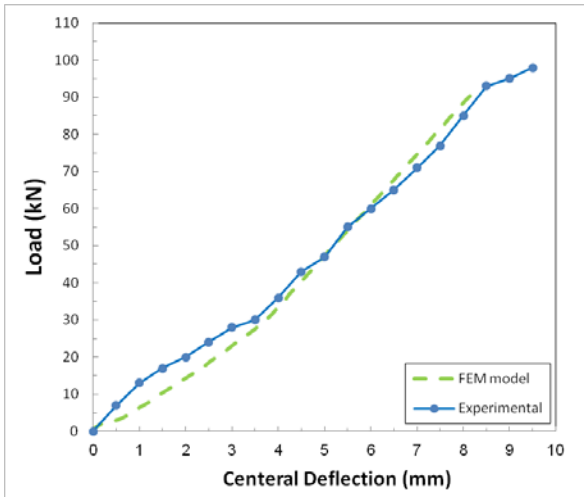

Slab S22

Figure (7)Abdulhameedslabs, experimental and numerical load- deflection curves.

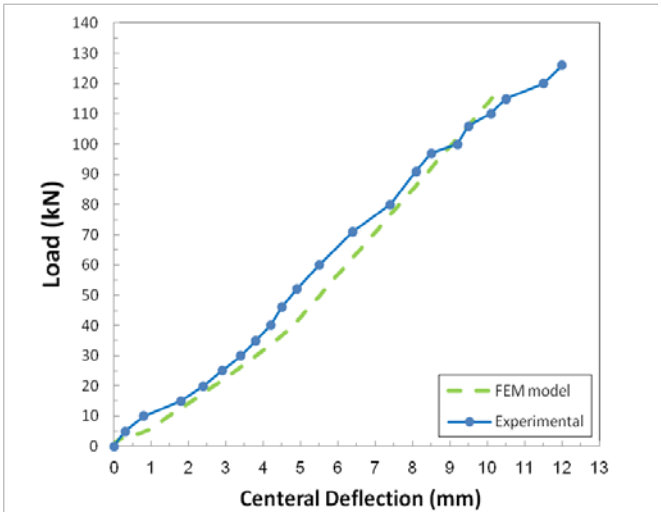

Slab S23

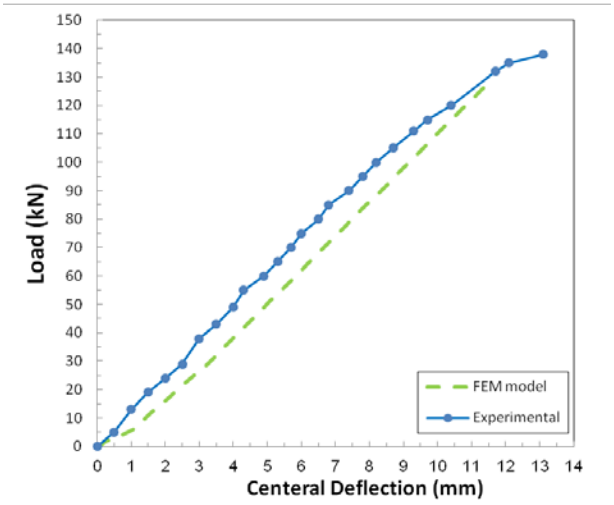

Slab S24

Figure (8)Abdulhameedslabs, experimental and numerical load- deflection curves.

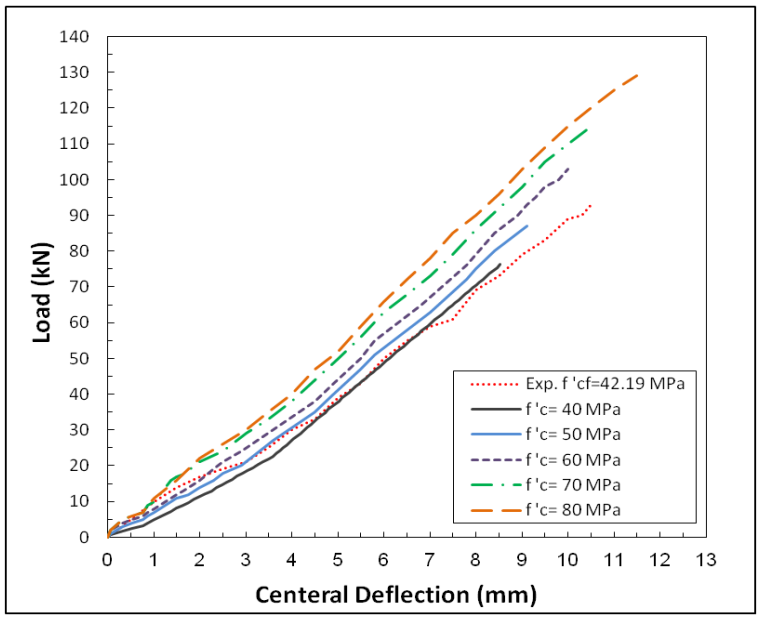

Figure (9) Influence of concrete compressive strength (f'_c) on theload-deflection behavior of slabS21 (V_f=0.0%).

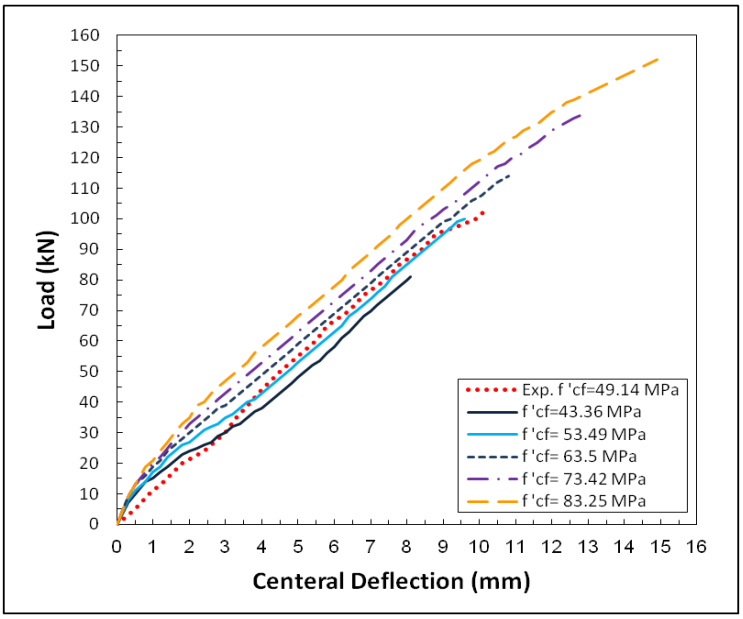

Figure (10) Influence of concrete compressive strength (f'_{cf}) on the load-deflection behavior of slab S12 (V_f=0.5%).

Influence of Fiber Content

The presence of fibers enhances the stiffness, ductility and ultimate shear capacity of high strength steel fiber reinforced concrete slabs. In order to do this verification, slab S21 (without fibers) was used for this study. The slab has been analyzed by using different amounts of steel fibers of V_f = 0.0, 0.5, 1.0, 1.5, and 2.0%. The numerical results of this analysis are listed in Table (7). The finite element analysis for slab S21 reveals that the stiffness, ductility and ultimate shear capacity are significantly increased due to presence of steel fibers, as shown in Fig. (11).

Influence of Amount of Steel

Fig. (12) shows the effect of using different amounts of reinforcement on the load-deflection behavior of slab (S12) . Selected steel ratios were 0.26, 1, 1.5 and 2% . The finite element solutions indicated that the post-cracking stiffness and the ultimate shear capacity are increased with the increase in the amount of steel. It can be noted that the deflection of the slab at the ultimate load was decreased with increasing the amount of steel. The numerical results of this analysis are listed in Table (8). The finite element analysis indicated that the ultimate load capacity is increased by about (57%) when the steel ratio is increased by (50%).

Influence of Slab Depth

To study the influence of using different slab thicknesses on the behavior of high strength steel fiber reinforced concrete slabs, Slab S12 was numerically analyzed by FEM with three different values of slab thickness. The chosen thicknesses were 45, 60 and 75 mm. The load-deflection curves obtained from the finite element analysis together with the experimental result (slab thickness equals to 60 mm) are shown in Fig. (13). The finite element results reveal that a considerable increase in the ultimate load capacity has been achieved by increasing the slab thickness. The FEM results of this analysis are listed in Table (9). It can be noted that increasing the slab thickness by 25% leads to an increase the ultimate load by about 19%, while decreasing the thickness to 25% leads to a decrease in the ultimate load by about 22%.

Table (7) Influence of fiber content on the ultimate load of slab S21

Fiber content V_f %	0.0	0.5	1.0	1.5	2.0
FEM ultimate load V_u(kN)	84.34	93.42	112.23	128.56	153.21
% Increase in ultimate load	**Reference**	10.77	33.07	52.43	81.65
Final deflection (mm)	9.21	9.5	10.63	12.31	10.45

Table (8) Influence of amount of steel on the ultimate load of slab S12

Steel ratio %	FEM		Exp.	FEM	
	0.26	1	1.5	1.5	2
Ultimate load (kN)	39.97	75.26	102.5	91.91	118.65
Final deflection (mm)	13.74	11.03	10.20	8.88	8.02

Table (9) Influence of depth of slab on the ultimate load of slab S12

Depth of slab (mm)	FEM	Exp.	FEM	
	45	60	60	75
Ultimate load (kN)	71.68	102.5	91.91	109.52
Final deflection (mm)	11.82	10.20	8.88	6.23

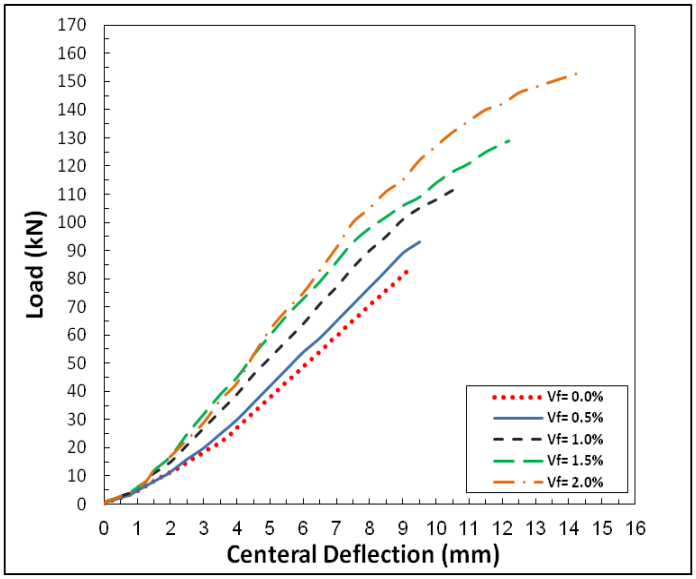

Figure (11) Influence of fiber content on the load-deflection behavior of slab S21.

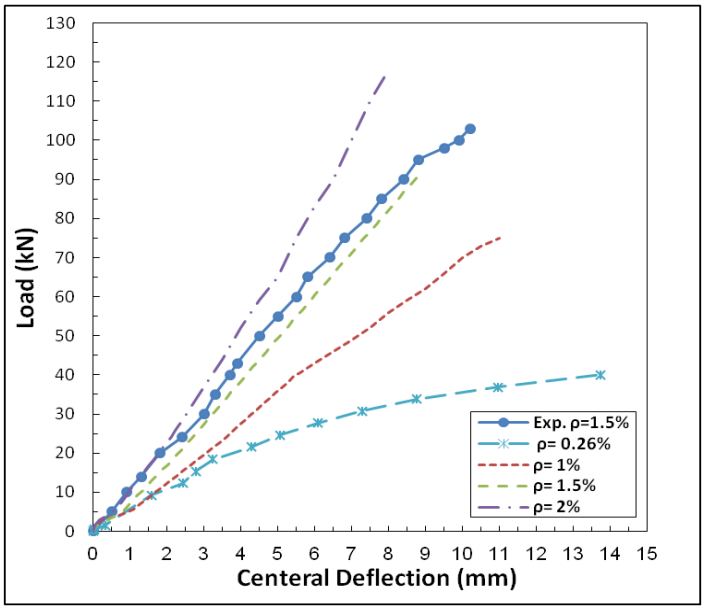

Figure (12) Influence of amount of steel on the load-deflection behavior of slab S12.

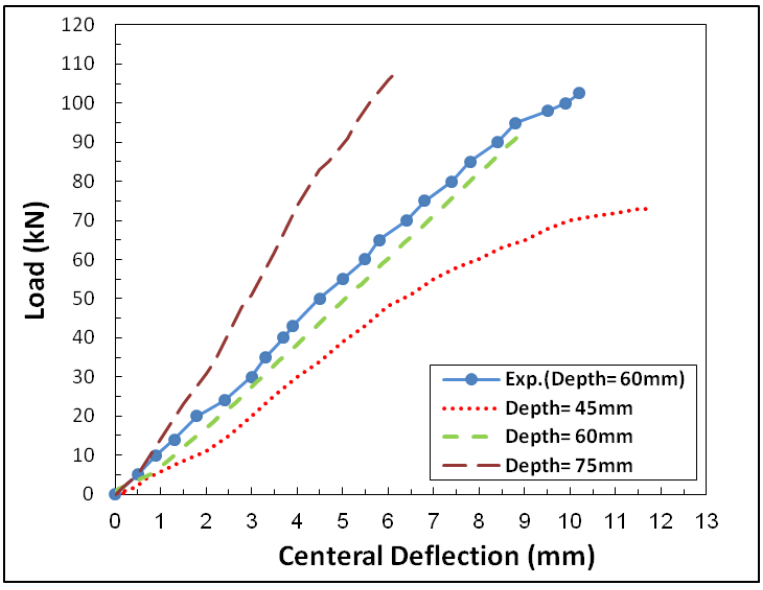

Figure (13) Influence of depth of slab on the load-deflection behavior of slab S12.

CONCLUSIONS

1- The three-dimensional nonlinear finite element model used in the present research work is able to simulate the behavior of high strength steel fiber reinforced concrete slabs. The finite element analysis showed that the predicted behavior and the ultimate load capacity are in accepted agreement with the experimental results**.**

2- The predicted ultimate load capacity of slabs was found to be depending on the grade of concrete. The finite element analyses carried out for compressive strength ranging from 40 to 80 MPa indicated that the percentage increase in ultimate load capacity is about 69% and 84% for slabs without and with 0.5% steel fibers, respectively.

3- The ultimate load capacity of the analyzed slabs is significantly increased with the addition of steel fibers compared to slabs without steel fibers, the ultimate load capacity increased by about 10.77%, 33.07%, 52.43% and 81.65% for fiber contents of 0.5%, 1.0%, 1.5% and 2.0%, respectively.

4-The finite element solutions reveal that the ultimate load of slabs is increased with the increase of the amount of reinforcement, when the steel ratio is increased by about 50%, an increase in the ultimate load capacity by 57% is achieved.

5-The finite element analyses results show that the increasing of slab thickness from 60 to 75 mm leads to an increase in the ultimate load by about 19%, while decreasing the thickness of slab from 60 to 45 mm leads to a decrease in the ultimate load by about 22%.

REFERENCES

[1]Ying, T.," Behavior and Modeling of Reinforced Concrete Slab-Column Connections,"Ph.D. Thesis, The University of Texas at Austin, May, 2007, 231p.

[2]Ngo, T., "Punching Shear Resistance of High-Strength Concrete Slabs," Electronic Journal of Structural Engineering, Vol. 1, No. 1, 2001, pp. 52-59.

[3]Abdulhameed A. Yaseen, "Punching Shear Strength of Steel Fiber High Strength Reinforced Concrete Slabs," M.Sc. Thesis, Department of Civil Engineering ,University of Salahaddin, 2006, 111p.

[4]Swamy R. N., and Ali S. A. R. ,"Punching Shear Behavior of Reinforced Slab–Column Connections Made with Steel Fiber Concrete, "ACIStructural Journal, Vol. 79, No. 6, 1982, pp. 392–406.

[5]Li, V. C., " Large Volume, High-Performance Applications of Fibers in Civil Engineering," ACE-MRL, Department of Civil and Environmental Engineering, University of Michigan, Ann Arbor, November, 2000, pp. 660-676.

[6]Shah, R. H., "Crack and Deformation Characteristics of SFRC Deep Beams," IE (I) Journal-CV, Vol. 85, May, 2004, pp. 44-48.

[7]Thannon, A. Y.,"Ultimate Load Analysis of Reinforced Concrete Stiffened Shells and Folded Slabs Used in Architectural Structures", Ph.D. Thesis, University of Wales, Swansea, 1988.

[8]Hinton, E. and Owen, D.R.J., "Finite Element Software for Plates and Shells", Pineridge Press, Swansea, 1984.

[9]Allose, L. E., "Three Dimensional Nonlinear Finite Element Analysis of Steel Fiber Reinforced Concrete Beams in Torsion", M.Sc. Thesis, University of Technology, 1996.
[10]Abdul-Wahab H.M.S., "Strength of reinforced concrete corbels with fibers ", ACI Structure J.,Vol.86,No.1, Jan.-Feb., 1989,pp.60-66.
[11]Al-Shaarbaf , I. A. S., "Three-Dimensional Nonlinear Finite Element Analysis of Reinforced Concrete Beams in Torsion,"Ph.D Thesis. University of Bradford , 1990, 323p.
[12]Al-Mousely B. S. T.,"Three-Dimensional Non-Linear Finite Element Analysis For Steel Fiber Reinforced Concrete Beam Subjected to Combined Bending and Torsion," M.Sc. Thesis, University of Technology, Baghdad,1998, 122p.
[13]Naji, J. H., and I.May, "The Effect of Some Numerical and Material Parameters on the Nonlinear Finite Element Analysis of Reinforced Concrete Beams", Proceedings of the Third Arab Engineering Conference, Vol. 1, March 1998, No. 5 , pp. 10-17.
[14]Al-Azzawi , Z. M. K. , "Capacity of High Strength Fiber Reinforced Beam Column Joints ", M. Sc. Thesis, University of Technology, 1997.
[15]Bunni, Z. J.,"Shear Strength in High-Strength Fiber Reinforced Concrete Beams," M. Sc. Thesis, University of Technology, Baghdad, 1998, 105p.
[16]Wafa, F. F. and Ashour, S. A.,"Mechanical Properties of High Strength Fiber Reinforced Concrete," ACI Material Journal, Vol. 89, 1992, No. 5, pp. 499-455.
[17]Carrasquillo, R. L., Nilson, A. H. and Slate, F. O., "Properties of High Strength Concrete Subject to Short-Term Loads," ACI Journal, Vol. 78, No.3, May-June 1981, PP. 171-178.
[18]Shah, S. P. and Rangan, B. V.,"Fiber Reinforced Concrete Properties," ACI Journal, Vol. 68, No.2, Feb. 1971, pp. 126-135.